Short Communication

Avicenna Journal of Medical Biotechnology
Volume 17, Issue 4, 303-311
https://doi.org/10.18502/ajmb.v17i4.20076

Check for updates

Dual-Modality Therapy: Synergistic Enhancement of Radio-Hyperthermia by Gold-Gold Sulfide Nanoparticles in MCF-7 Cells

Mahdi Sadat-Darbandi [1], Amirhossein Fathabadi [2,3], Shabnam Oloomi [4*] and Ameneh Sazgarnia [2,5*]

1. Department of Medical Physics, Reza Radiotherapy and Oncology Center, Mashhad, Iran
2. Department of Medical Physics, Faculty of Medicine, Mashhad University of Medical Sciences, Mashhad, Iran
3. Student Research Committee, Mashhad University of Medical Sciences, Mashhad, Iran
4. Department of Radiology Technology, School of Paramedical and Rehabilitation Sciences, Mashhad University of Medical Sciences, Mashhad, Iran
5. Medical Physics Research Center, Basic Sciences Research Institute, Mashhad University of Medical Sciences, Mashhad, Iran

*** Corresponding authors:**
Ameneh Sazgarnia, Ph.D., Department of Medical Physics, Faculty of Medicine, Mashhad University of Medical Sciences, Mashhad, Iran

Shabnam Oloomi, Ph.D., Department of Medical Physics, Faculty of Medicine, Mashhad University of Medical Sciences, Mashhad, Iran
Tel: +98 9153156585, 9155149930
Fax: +98 51 38846710-34
E-mail: SazgarniaA@mums.ac.ir
OlumiSh@mums.ac.ir
Received: 2 Feb 2025
Accepted: 9 Jun 2025

Abstract

Background: This study examines the synergistic impact of Gold-Gold Sulfide (GGS) nanoparticles combined with hyperthermia and radiotherapy on MCF-7 cancer cells. GGS nanoparticles, with strong near-infrared absorption and photothermal properties, enhance cellular sensitivity to radiotherapy.

Methods: MCF-7 cells were treated with varying GGS concentrations and exposed to radiation doses of 50, 100, and 200 *cGy*, alongside laser irradiation for 10, 40, and 80 *s*. The IC_{50} for GGS nanoparticles was approximately 350 μM.

Results: Results revealed a significant reduction in cell viability with the combined GGS and laser exposure ($p<0.001$), demonstrating a synergistic effect in a dose-dependent manner. Further enhancement in cell viability reduction was observed when GGS nanoparticles were combined with both hyperthermia and radiotherapy ($p<0.01$).

Conclusion: These findings suggest that GGS nanoparticles offer greater efficacy and reduced toxicity compared to gold nanoparticles, highlighting their potential for improving cancer therapy outcomes through combined hyperthermic and radiotherapeutic approaches.

Keywords: Combined modality therapy, Hyperthermia, Induced, Metal nanoparticles, MCF-7 cells, Radiotherapy
To cite this article: Sadat-Darbandi M, Fathabadi Ah, Oloomi Sh, Sazgarnia A. Dual-Modality Therapy: Synergistic Enhancement of Radio-Hyperthermia by Gold-Gold Sulfide Nanoparticles in MCF-7 Cells. Avicenna J Med Biotech 2025;17(4):303-311.

Introduction

Breast cancer is the most prevalent cancer in women and a significant global health burden [1]. With approximately one in seven women diagnosed in their lifetime [2], relapse and metastasis remain critical challenges despite treatment advances [3]. Radiotherapy, a cornerstone of breast cancer treatment often used post-surgery [4,5], faces limitations including dose restriction due to adjacent healthy tissues, cancer cell radioresistance, tumor recurrence, and adverse effects [6]. Additionally, radiotherapy primarily targets G2- and M-phase tumor cells, demonstrating minimal impact on hypoxic cells and those in the S phase of the cell cycle; therefore, it plays a crucial role in the recurrence and development of life-threatening metastases after radiation therapy [7].

Hyperthermia, elevating tumor temperature (typically 42-45°*C*), has emerged as a promising adjuvant therapy [8], exploiting the greater thermosensitivity of malignant tissues. Elevated temperatures (41.5-42.5°*C*) can induce cytotoxicity and vascular damage in tumors, particularly in acidic and hypoxic environments [9].

Many studies have shown that combining hyperthermia with radiotherapy yields a notable advantage owing to its synergistic effects. Hyperthermia enhances tumor oxygenation and vascular permeability [6], increasing cancer cell radiosensitivity [10]. This synergy includes cell-cycle complementarity, as hyperthermia targets S-phase cells relatively resistant to radiotherapy [11]. Despite its potential benefits, hyperthermia has

This work is licensed under a Creative Commons Attribution–NonCommercial 4.0 International License.

some limitations. One of the main challenges is the lack of selectivity in the heating process, as both normal and cancer cells absorb heat, leading to potential side effects and damage to the surrounding healthy tissues. Furthermore, the thermal effects of hyperthermia are typically limited to short durations, and sustained heating can take time to achieve [12].

Nanotechnology, particularly using nanoparticles like gold (AuNPs), offers strategies to improve cancer therapies [13]. AuNPs, with their high atomic number (Z=79), significantly enhance radiation dose deposition ($\sigma ph \propto (Z/E)^3$) *via* surface plasmon resonance, generating Auger electrons, increasing Reactive Oxygen Species (ROS), DNA damage, and apoptosis [14]. Their optical and electronic properties also make AuNPs ideal for photothermal therapy [15], efficiently converting Near-Infrared (NIR) light to heat, causing protein denaturation and mitochondrial dysfunction *via* ROS [16]. Passive accumulation of AuNPs in tumors through the Enhanced Permeability and Retention (EPR) effect enhances treatment outcomes and reduces side effects, ultimately improving patient survival rates [17]. Additionally, AuNPs exhibit excellent biocompatibility, and their synthetic versatility allows convenient customization options [18] (Scheme 1).

Gold-Gold Sulfide (GGS) nanoshells, featuring a gold core and gold sulfide shell, exhibit strong NIR absorption ideal for deep-tissue penetration in therapy and imaging [19]. NIR irradiation induces localized hyperthermia and cell death through photothermal conversion, damaging membranes, proteins, and triggering apoptosis *via* ROS [20]. Elevated ROS also induce oxidative stress, disrupting mitochondrial function and cell cycle, while GGS nanoparticles may impair DNA repair mechanisms like homologous recombination, increasing radiosensitivity [21]. GGS nanoshells offer reduced toxicity compared to gold-silicon counterparts due to their smaller size and surface chemistry [9], facilitating biological navigation, cellular uptake, and EPR-mediated tumor accumulation. They also serve as dual therapeutic and imaging agents [22]. Favorable pharmacokinetics and *in vivo* stability are crucial for clinical translation, with recent studies showing promising circulation times and biodistribution profiles [23].

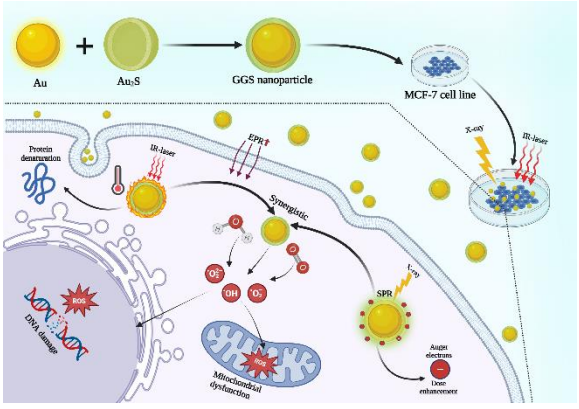

Scheme 1. Mechanism of Action of GGS Nanoparticles in Combination with Hyperthermia and Ionizing Radiation in MCF-7 Cells.

Given the demonstrated benefits of combining hyperthermia and radiotherapy with nanoparticle-based approaches [10,24-27], this study aimed to investigate the combinatorial therapeutic effects of GGS nanoparticles with hyperthermia and radiotherapy in breast cancer.

Materials and Methods

Materials

Gold (III) chloride trihydrate ($HAuCl_4$, 3H2O) was obtained from the American company of Alfa Aesar, and $Na_2S_2O_3$ and Polyvinyl pyrrolidone (PVP-40) were purchased from Merck (Germany). Trypan blue, 3-(4,5-dimethylthiazol-2-yl)-2,5-diphenyltetrazolium bromide (MTT), dimethyl sulfoxide (DMSO), streptomycin, penicillin, and trypsin–ethylene diamine tetra acetic acid (EDTA) were purchased from Sigma-Aldrich Company (St. Louis, MO, USA). Fetal Bovine Serum (FBS) and Roswell Park Memorial Institute (RPMI) 1640 cell culture medium were purchased from Gibco (USA). The human breast cancer MCF-7 cell line was obtained from the Pasteur Institute of Iran (Tehran, Iran).

Synthesis and characterization of GGS-NPs

GGS nanoconjugate was prepared according to the procedure described by Day *et al* [28]. Briefly, an aqueous solution of 2000 μM $HAuCl_4$ (Au; 150 *ppm*) and 1000 μM $Na_2S_2O_3$ was mixed in small quantities at a 1:1 to 1:2 ($HAuCl_4$, $Na_2S_2O_3$) ratio range and stored at room temperature for one day. To achieve the required volumetric ratio, ensuring that the GGS nanoparticles resonate near the 800 *nm* wavelength, a UV-visible spectrophotometer (UV 1700, Shimadzu Corp., Japan) was used to record the absorption spectrum between 200–900 *nm* wavelengths. The reaction's endpoint was considered when an absorption peak at 808 *nm* was generated. After confirming the formation of GGS nanoparticles, 0.6 *g* of polyvinylpyrrolidone (PVP-40; $(C_6H_9NO)_n$) was added to the mixture to prevent nanoparticle aggregation. To purify the nanoparticles, sequential centrifugation was performed at 12,000 *rpm* for 20 *min*. The purity of GGS nanoshells was confirmed by UV-Vis spectroscopy and dynamic light scattering (Zetasizer, Malvern Inc., USA) to determine the size distribution and remove any impurities or aggregates.

Cell culture

MCF-7 cells were cultured as a monolayer using RPMI-1640 medium supplemented with 10% FBS, penicillin (100 *unit/ml*), and streptomycin (100 $\mu g/ml$) in 75 cm^3 flasks. Cells were incubated in a humidified atmosphere containing 5% CO_2 at 37°*C*. For all experiments, cells were seeded at a density of 5×10^5 *cells/ml*, and each experimental condition was performed in triplicate to ensure reproducibility. Fresh medium was provided every three days.

Cytotoxicity of GGS

The cytotoxicity of a core-shell nano complex was assessed by evaluating the viability of cells incubated with different concentrations of nanoparticles. The assessment was carried out using the MTT tetrazolium assay. This method measures the capability of metabolically active mitochondria in live cells to convert a colorless tetrazolium compound into a blue formazan product. To perform this assay, the MCF-7 cell suspensions (5×10^5 *cells/ml*) were seeded in a 96-well plate and, 24 *hr* later, were treated with different concentrations of GGS (0, 50, 100, 200, 300, and 400 μM). After two *hr*, the nano complex was removed, and cells were washed with PBS to remove the remaining GGS [9,29]. MTT assay was performed 24 *hr* post-treatment. After adding 100 μl of FBS-free culture medium, 10 μl of MTT dye (5 *mg/ml* in PBS) was added to each well, and the plate was incubated for 4 *hr*. Then, the media was removed from the wells, and the cells were lysed with DMSO (10 μl per well). The samples' Optical Density (OD) was measured at 545 *nm* using an ELISA reader (Stat Fax-2100 Awareness, Mountain View, CA, USA). Dissolved formazan's OD is directly proportional to living cells. Cell viability was calculated as follows [30]. All experiments were repeated at least three times:

$$\text{cell viability (\%)} = \frac{\text{Optical density value of test}}{\text{Optical density value of control}} \times 100$$

Infra-red irradiation

Infra-Red (IR) irradiation was performed by a continuous laser beam at a wavelength of 808 *nm* (Optilas model MDL-III-808-2.5W, Changchun New Industries Optoelectronics Technology Co., Ltd., Changchun, China) with 5×8 mm^2 spot size. The MCF-7 cells were cultured at a 5×105 *cells/ml* density at 96-well tissue plates. After 24 *hr*, the cells were incubated with different concentrations of GGS (0, 50, 150, and 200 μM) for 2 *hr*. After cell washing with FBS, their laser irradiation was performed for 10, 40, and 80 *s*. Temperature variations were recorded by a thermo-vision camera (TESTO-882, Hampshire, UK). Finally, the cell cultures were continued for five days before the MTT assay was performed.

X-ray irradiation

A surface X-ray tube with a 20 cm^2 cone beam and radiation condition of 100 kV_p and 80 *mA* with a 1229.5 *cGy/min* dose rate was used. Cells received exposure from the posterior at 100 *cm* from the bottom of the plate with the 40×40 *cm* radiation field size. After cell washing, ionization radiation was performed at 50, 100, and 200 *cGy* on cell cultures with different concentrations of GGS (0, 50 μM), and five days later, the MTT assay was performed.

X-ray and infra-red exposure

To investigate the combined impact of radiotherapy and hyperthermia (with and without GGS), The MCF-7 cells were cultured in a 96-well plate and maintained in an incubator for 24 *hr*. After removing the culture medium, GGS nanoparticles were added to each well in different concertation (50, 150 μM), and cells were maintained in an incubator. Two *hr* later, the cell cultures were exposed to a laser beam at different time durations of 1, 2, and 4 *min*. Subsequently, the cells were immediately exposed to 200 *cGy* X-ray radiation (the average time between IR and X-ray exposure was less than 10 *min*). Afterward, the cells were left to incubate for an additional five days before the MTT assay.

Statistical analysis

Statistical analysis was performed using the GraphPad Prism 9 software (GraphPad Software, Inc., San Diego, CA). A one-way ANOVA and Tukey test were used to evaluate the significance of the results. The $p<0.05$ was considered as significant.

Results

GGS characterization

Figure 1A shows the Particle Size Analysis (PSA) performed using Dynamic Light Scattering (DLS), which revealed a dominant particle size of 5.4 *nm*. The Polydispersity Index (PDI) was measured at 0.63, indicating a moderate level of size variation within the nanoparticle population. In addition, a Transmission Electron Microscopy (TEM) image of the synthesized GGS nanoparticles, shown in figure 2, confirms the structural morphology and uniformity of the nanoshells, further validating the size distribution observed in the DLS analysis. In the UV-Vis spectroscopy analysis, shown in figure 1B, the synthesized GGS nanoparticles exhibited two distinct absorption bands.

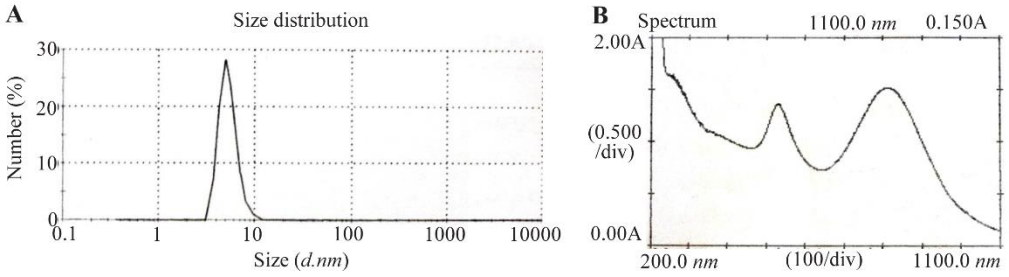

Figure 1. A) Size distribution of synthesized gold- gold sulfide nanoshells (maximum abundance of particles distribution at 5.4 *nm*), B) extinction spectrum of the GGS-NPs (two absorption peaks at 530 and 814 *nm*).

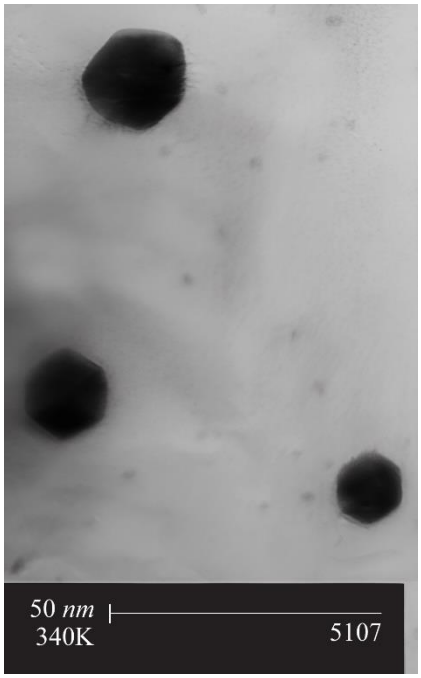

Figure 2. TEM image of synthesized gold-gold sulfide nanoshells.

A prominent absorption peak was observed at 814 *nm* in the NIR region, which corresponds to the plasmon resonance of GGS nanoshells. This NIR peak is crucial for applications in photothermal therapy as it allows for deep tissue penetration, making GGS nanoparticles ideal for biomedical applications. The weaker absorption band at 530 *nm*, located in the visible region, is attributed to the SPR of the gold core. These findings are consistent with previous reports on the optical properties of gold-gold sulfide nanoshells [28,31]. The strong absorption in the NIR region, coupled with the secondary peak in the visible range, confirms the successful synthesis of GGS nanoparticles with the desired optical properties for synergistic radio-hyperthermia applications.

Cytotoxicity of GGS on MCF-7 cells

To ensure the suitability of synthesized nanomaterials for biomedical applications, it is essential to evaluate their cytotoxicity. Figure 3A illustrates the viability assessment of MCF-7 cells incubated with varying concentrations of GGS nanoparticles. The data reveals that MCF-7 cell viability declined by over 20% at concentrations above 200 μM. The half-maximal inhibitory concentration (IC_{50}) of the GGS nanoparticles was determined to be approximately 350 μM. This IC_{50} value represents the concentration required to inhibit 50% of cell viability when GGS is used as a monotherapy. However, in the combination treatments involving hyperthermia and radiotherapy, lower concentrations of GGS nanoparticles (50-200 μM) were used, as these concentrations were sufficient to enhance the therapeutic effects without reaching cytotoxic levels.

Thermometry findings

Temperature monitoring of GGS nanoparticles at different concentrations in a liquid medium during NIR-Laser exposure showed the strong light-absorption capability of GGS nanoshells figure 3B. Increasing the GGS concentration for shorter durations (1 and 2 *min*) resulted in a significant rise in temperature. However, this effect weakened after 4 *min* of exposure.

Photothermal effect

The effects of GGS NPs on hyperthermia efficacy were investigated by exposing MCF-7 cells to NIR lasers at varying concentrations. As depicted in figure 4A, combining GGS nanoparticles with laser exposure substantially reduced cell viability. However, no significant effect on cell viability was observed when the exposure time was increased to 80 *s*. Furthermore, increasing the concentration of GGS nanoparticles from 150 μM to 200 μM did not lead to any significant differences in cell viability.

X-ray treatment

In addition, the radio sensitizing effects of GGS nanoparticles were investigated (Figure 4B). The results demonstrated a dose-dependent increase in the synergistic effect of GGS nanoparticles and X-ray irradiation. A significant difference was observed between the two groups at a dose of 200 *cGy*.

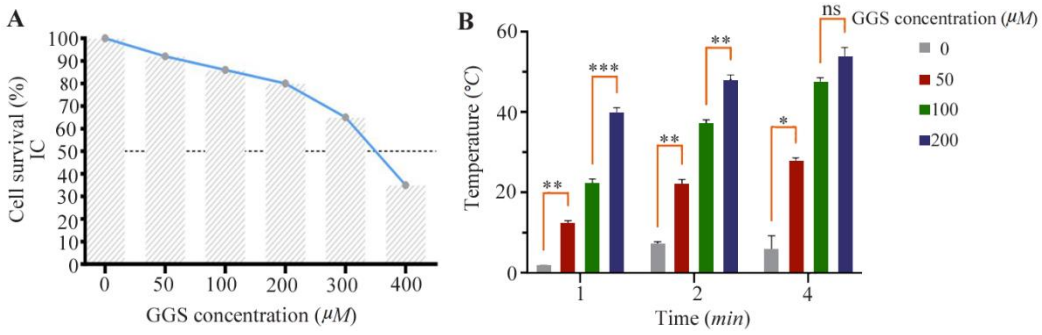

Figure 3. A) MCF-7 cells viability treated with different concentrations of GGS nanoparticles (incubation time: 2 *hr*), B) Temperature rise profile of GGS nanoparticles at different concentrations upon administration of NIR laser (808 *nm*; 2.5 W/cm^2) in an aqueous medium; ns stands for not statistically significant, *p<0.05, **p<0.01, and ***p<0.001.

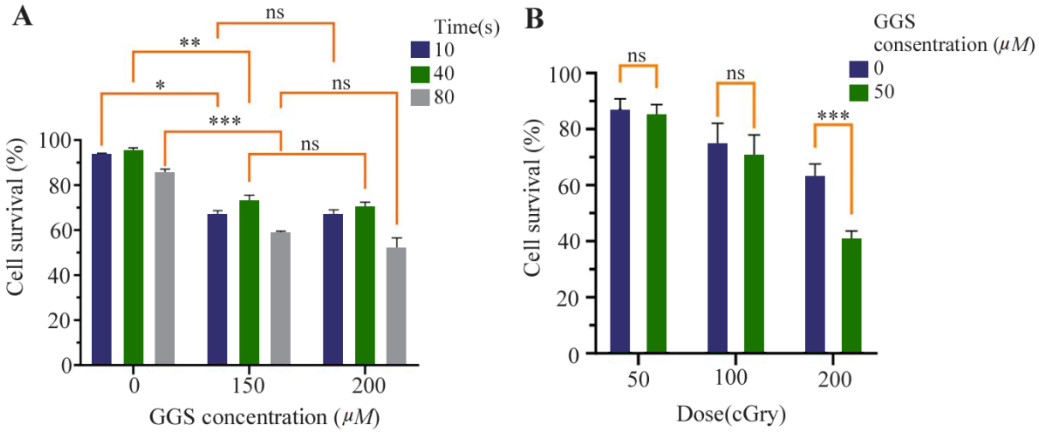

Figure 4. A) The viability of MCF-7 cells treated with GGS concentrations and then exposed to NIR Laser in a time-dependent manner, B) The viability of MCF-7 cells treated with GGS NPs and then exposed to different doses of X-ray radiation; ns stands for not statistically significant, *p<0.05, **p<0.01, ***p<0.001, and ****p<0.0001.

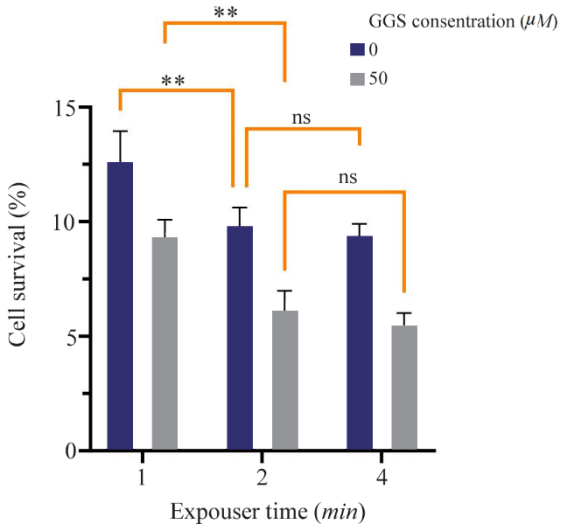

Figure 5. The MCF-7 cells viability after receiving combination therapy (2 Gy X-ray radiation, NIR laser (808 *nm*; 2.5 W/cm^2), and GGS nanoparticles); ns stands for not statistically significant, **p<0.01.

Combinatory treatments

Figure 5 illustrates the combinatorial effects of radiotherapy, hyperthermia, and GGS nanoparticles. These findings demonstrated that the combination of hyperthermia and X-ray radiation in the presence of GGS nanoparticles significantly reduced cell viability compared to the combination of hyperthermia and X-ray radiation alone. However, no significant reduction in cell viability was observed when the laser exposure time was increased from 2 to 4 *min*.

Discussion

Nanoparticles, with their unique physicochemical properties, have catalyzed significant advancements across various medical disciplines. This study investigated the potential of GGS nanoparticles to enhance the efficacy of radiotherapy and hyperthermia in a multifaceted therapeutic approach against MCF-7 breast cancer cells. The present study findings demonstrate that GGS nanoparticles, primarily owing to their small size and efficient Near-Infrared (NIR) absorption, offer distinct advantages that can substantially improve therapeutic outcomes when combined with these established modalities.

The GGS nanoparticles synthesized herein exhibited a mean diameter of 5.4 *nm* (Figure 1A and Figure 2), a characteristic that confers several potential benefits. While the observed PDI of 0.63 indicates moderate size variation, a characteristic not uncommon for such synthesis methods, future refinement through techniques like size-selective centrifugation could improve uniformity and potentially enhance therapeutic consistency [32]. Nevertheless, compared to larger constructs such as 100-200 *nm* Gold-Silica Nanoshells (GSNs), these smaller GGS nanoparticles are associated with simplified manufacturing, and may offer improved biodistribution and deeper tumor penetration [33]. Their reduced dimensions could also facilitate evasion of rapid clearance by the Mononuclear Phagocyte System (MPS), potentially extending systemic circulation time [33].

A central rationale for focusing on GGS nanoparticles lies in their inherent advantages over some conventional gold-based nanomaterials for photothermal and radiosensitizing applications. GGS nanoshells are engineered for superior NIR absorption; literature suggests efficiencies approaching 98-99% at their resonant wavelength, often exceeding that of GSNs (typically 67-85%) or solid gold nanospheres which may have less optimal absorption profiles in the NIR-I window [9, 34,35]. This enhanced photothermal conversion, coupled with their small size facilitating cellular uptake and tumor penetration [33], likely underpins the potent cytotoxic and synergistic effects observed in this study. Indeed, previous *in vivo* studies have indicated that PEGylated GGS nanoparticles can achieve longer cir-

culation times compared to GSNs [28,36], suggesting better tumor accumulation via the EPR effect. In the context of radiosensitization, while gold's high atomic number intrinsically contributes to localized radiation dose enhancement, the efficient uptake and potential for GGS nanoparticles to promote ROS generation may further augment this effect compared to other gold nanostructures whose efficacy can vary with physicochemical properties [20,21].

Cytotoxicity assessment is crucial for evaluating the clinical translational potential of any nanomaterial.[37] Our MTT assays revealed a dose-dependent decrease in MCF-7 cell viability upon GGS nanoparticle exposure, with an IC50 of approximately 350 μM (Figure 3A). This cytotoxicity is likely mediated, at least in part, by ROS generation leading to oxidative stress and subsequent apoptosis [38,39], a mechanism reported for other gold-based and metallic nanoparticles [40,41]. It is noteworthy that while some nanoparticles like silver nanoparticles (AgNPs) exhibit pronounced cytotoxicity *via* excessive ROS production and membrane disruption [42], Ramezanzadeh *et al* reported that coating GGS nanoparticles with cetuximab, an EGFR-targeting antibody, increased cell viability (by approximately 20%) across various GGS concentration [29]. Our use of uncoated GGS nanoparticles allowed for assessment of their intrinsic effects. Discrepancies in reported cytotoxicity, such as the 5% cell survival reduction in another GGS study [43], can often be attributed to variations in nanoparticle concentration and, critically, incubation duration. Present study 2 *hr* incubation, compared to a 40-*min* period in the aforementioned study, likely permitted greater nanoparticle-cell interaction and subsequent effects, underscoring the need for standardized protocols in comparative nanoparticle research.

The combination of GGS nanoparticles (150 μM) with laser-induced hyperthermia significantly reduced cell viability (Figure 4A). However, a plateau effect was observed, where further increases in GGS concentration (*e.g.*, to 200 μM) or extending laser exposure from 40 to 80 *s* did not always yield a proportionally greater cytotoxic effect. This saturation in photothermal response could be attributed to cellular protective mechanisms, such as the upregulation of Heat Shock Proteins (HSPs), which confer thermotolerance [12]. Consistent with the present study findings, Ramezanzadeh *et al* also reported no significant difference in cell viability between GGS concentrations of 200 μM and 250 μM [29], further supporting the idea of a saturation effect. Comparatively, Mohammadi *et al* [44] reported a 40% reduction in MCF-7 cell viability after a 10 *min* laser exposure with other gold nanoparticles. The present study achieved a similar reduction with a significantly shorter 80 *s* exposure, suggesting GGS nanoparticles possess superior photothermal conversion efficiency, attributable to their optimized NIR absorption properties [45,46].

Furthermore, GGS nanoparticles (50 μM) demonstrably enhanced radiation efficacy at 200 *cGy*, resulting in a 23.5% greater reduction in cell viability compared to radiation alone (Figure 4B), consistent with the known radiosensitizing properties of gold-based nanoparticles [47]. A threshold effect was apparent, as no significant radiosensitization was observed at lower radiation doses. While other gold nanostructures like nanospheres [48] and nanorods [49], also exhibit radiosensitization, direct comparisons under standardized conditions are necessary to definitively ascertain the relative radiosensitizing capacity of GGS nanoparticles.

The triple combination of 200 *cGy* X-ray radiation, GGS-mediated hyperthermia, and GGS nanoparticles yielded the most profound cytotoxic effect, with up to a 95% reduction in cell viability after 2 and 4 *min* of laser exposure (Figure 5). Interestingly, extending laser exposure from 2 to 4 *min* in these combination groups did not significantly further decrease cell viability, suggesting that a 2-minute hyperthermia session was sufficient to achieve maximal synergy under these conditions. This outcome is notably more effective than a previous study using different gold nanoparticles, which reported an approximately 85% reduction in cell viability after a 10 *min* laser exposure combined with 200 *cGy* radiation [44]. This comparison suggests that GGS nanoparticles may offer enhanced synergistic efficacy with substantially shorter hyperthermia durations.

While this study utilized uncoated GGS nanoparticles to assess their intrinsic therapeutic properties, successful clinical translation necessitates addressing challenges such as opsonization, non-specific interactions, and rapid clearance. Surface functionalization strategies, such as PEGylation, can improve colloidal stability, prolong systemic circulation by reducing immune recognition, and potentially enhance tumor accumulation *via* the EPR effect, as demonstrated for PEGylated GGS [28,36]. Moreover, conjugating targeting ligands could enable active targeting to cancer cells, thereby increasing therapeutic specificity and minimizing off-target effects [40]. Future development of these GGS nanoparticles should therefore explore various surface engineering approaches to optimize their pharmacokinetic profiles and tumor-targeting capabilities.

Transitioning these promising *in vitro* findings to *in vivo* applications involves navigating further complexities. Optimizing pharmacokinetics and biodistribution is paramount to ensure adequate tumor accumulation of GGS nanoparticles, while minimizing systemic toxicity. Although the small size of GGS nanoparticles may inherently favor prolonged circulation and EPR-mediated tumor targeting, factors like protein corona formation and MPS uptake remain critical considerations [23]. Nanoparticle clearance mechanisms (*e.g.*, renal or hepatobiliary) must be understood to predict long-term fate and potential toxicity. Given the heterogeneity of the tumor microenvironment and the EPR effect,

passive targeting alone may be insufficient, potentially requiring active targeting strategies for enhanced specificity and efficacy. Consequently, comprehensive *in vivo* studies in relevant animal models are essential to meticulously evaluate these parameters, assess immunogenicity, define optimal therapeutic regimens, and confirm the long-term safety and efficacy of GGS-mediated dual-modality therapy.

This study, while providing compelling evidence for the synergistic potential of GGS nanoparticles, has certain limitations. Primarily, direct experimental validation of the precise molecular mechanisms (*e.g.*, apoptosis induction, ROS generation levels, DNA damage quantification) was not conducted. Although existing literature supports the involvement of these pathways [20,21], future work incorporating specific assays like Annexin V/PI staining, DCFDA for ROS, or γH2AX immunostaining is crucial for full mechanistic elucidation. Furthermore, this investigation was performed exclusively on the MCF-7 breast cancer cell line. A comprehensive assessment of the therapeutic index and potential off-target effects necessitates comparative studies using non-malignant human cell lines. While a range of concentrations and treatment durations were explored, a more exhaustive investigation could refine the understanding of dose-response relationships. These future studies will be pivotal in robustly validating and optimizing GGS nanoparticle-mediated dual-modality therapy for potential clinical application.

While this study provides compelling evidence for the potential of GGS nanoparticles in combined cancer therapy, it is important to acknowledge limitations. The study was conducted *in vitro* using a single breast cancer cell line (MCF-7), which limits the generalizability of the findings to other cancer types and *in vivo* conditions. Future studies should include a wider range of cell lines and, ultimately, *in vivo* models to validate these findings. Furthermore, while a range of concentrations and treatment durations were investigated, a more comprehensive investigation, including lower concentrations and shorter exposure times, could provide a more refined understanding of the dose-response relationship. Finally, while cell viability (MTT assay) was the primary endpoint, incorporating additional assays, such as flow cytometry for apoptosis analysis and assays to quantify ROS levels, would provide a more complete picture of the mechanisms underlying the observed effects.

Conclusion

This study demonstrates the potential of GGS nanoparticles to enhance the therapeutic effects of hyperthermia and radiotherapy. The observed reductions in cell viability and improved radiosensitization highlight their promise as a synergistic agent in combination cancer therapies. However, as these findings are based on *in vitro* experiments, further studies, including *in vivo* evaluations and long-term stability and toxicity assessments, are essential to validate their clinical applicability. With continued research, GGS nanoparticles could contribute to advancing cancer treatment strategies.

Acknowledgement

We confirm that the manuscript does not have an acknowledgement section.

Conflict of Interest

Authors declare no conflict of interest.

References

1. Mohamed WA, El-Nekhily NA, Mahmoud HE, Hussein AA, Sabra SA. Prodigiosin/celecoxib-loaded into zein/sodium caseinate nanoparticles as a potential therapy for triple negative breast cancer. Scientific Reports. 2024;14:181.
2. System NH. Breast cancer in women, https://www.nhs.uk/conditions/breast-cancer/
3. Khan MR, Alafaleq NO, Ramu AK, Alhosaini K, Khan MS, Zughaibi TA, et al. Evaluation of biogenically synthesized MgO NPs anticancer activity against breast cancer cells. Saudi Journal of Biological Sciences. 2024;31:103874.
4. Marques A, Belchior A, Silva F, Marques F, Campello MPC, Pinheiro T, et al. Dose Rate Effects on the Selective Radiosensitization of Prostate Cells by GRPR-Targeted Gold Nanoparticles. Int J Mol Sci. 2022;23:5279.
5. Abdollahi BB, Ghorbani M, Hamishehkar H, Malekzadeh R, Farajollahi A. Synthesis and characterization of actively HER-2 Targeted Fe3O4@ Au nanoparticles for molecular radiosensitization of breast cancer. BioImpacts: BI. 2023;13:17.
6. Neshastehriz A, Khosravi Z, Ghaznavi H, Shakeri-Zadeh A. Gold-coated iron oxide nanoparticles trigger apoptosis in the process of thermo-radiotherapy of U87-MG human glioma cells. Radiat Environ Biophys. 2018;57:405-418.
7. Kim JY, Lee WS, Seo SJ, Jung CW, Kim EH. Effects of gold nanoparticles on normal hepatocytes in radiation therapy. Transl Cancer Res. 2022;11:2572-2581.
8. Logghe T, Van Zwol E, Immordino B, Van den Cruys K, Peeters M, Giovannetti E, et al. Hyperthermia in combination with emerging targeted and immunotherapies as a new approach in cancer treatment. Cancers. 2024;16:505
9. Shahamat Z, Shokouhi M, Taheri AR, Eshghi H, Attaran-Kakhki N, Sazgarnia A. Induction of Localized Hyperthermia by Millisecond Laser Pulses in the Presence of Gold-Gold Sulphide Nanoparticles in a Phantom. Iranian Journal of Medical Physics. 2015;12:49-61.
10. Hadi F, Tavakkol S, Laurent S, Pirhajati V, Mahdavi SR, Neshastehriz A, et al. Combinatorial effects of radiofrequency hyperthermia and radiotherapy in the presence of magneto-plasmonic nanoparticles on MCF-7 breast cancer cells. J Cell Physiol. 2019;234:20028-20035.

11. Zhang A, Gao L. The Refined Application and Evolution of Nanotechnology in Enhancing Radiosensitivity During Radiotherapy: Transitioning from Gold Nanoparticles to Multifunctional Nanomaterials. Int J Nanomedicine. 2023;18:6233-6256.
12. Bala VM, Lampropoulou DI, Grammatikaki S, Koulo-ulias V, Lagopati N, Aravantinos G, et al. Nanoparticle-Mediated Hyperthermia and Cytotoxicity Mechanisms in Cancer. Int J Mol Sci. 2023;25:296.
13. Stephen ZR, Zhang M. Recent Progress in the Synergistic Combination of Nanoparticle-Mediated Hyperthermia and Immunotherapy for Treatment of Cancer. Adv Healthc Mater. 2021;10:e2001415.
14. Kazemzadeh A, Moradi H. A Monte Carlo Study on Dose Enhancement in the Presence of Nanoparticles by Photon Source: A Comparison between Various Concentration and Material of Nanoparticles. Frontiers in Biomedical Technologies. 2021;8:191-197.
15. Faid AH, Shouman SA, Badr YA, Sharaky M. Enhanced photothermal heating and combination therapy of gold nanoparticles on a breast cell model. BMC Chem. 2022;16:66.
16. Malekzadeh R, Mortezazadeh T, Abdulsahib WK, Babaye Abdollahi B, Hamblin MR, Mansoori B, et al. Nanoarchitecture-based photothermal ablation of cancer: A systematic review. Environ Res. 2023;236:116526
17. Mortezaee K, Narmani A, Salehi M, Bagheri H, Farhood B, Haghi-Aminjan H, et al. Synergic effects of nanoparticles-mediated hyperthermia in radiotherapy/ chemotherapy of cancer. Life Sci. 2021;269:119020.
18. D'Acunto M, Cioni P, Gabellieri E, Presciuttini G. Exploiting gold nanoparticles for diagnosis and cancer treatments. Nanotechnology. 2021;32:192001.
19. Ghorbani F, Attaran-Kakhki N, Sazgarnia A. The synergistic effect of photodynamic therapy and photothermal therapy in the presence of gold-gold sulfide nanoshells conjugated Indocyanine green on HeLa cells. Photodiagnosis Photodyn Ther. 2017;17:48-55.
20. Kepp O, Cerrato G, Sauvat A, Kroemer G. Nanoparticles releasing immunogenic cell death inducers upon near-infrared light exposure. 2022;11:2131227.
21. Liaw JW, Kuo CY, Tsai SW. The Effect of Quasi-Spherical Gold Nanoparticles on Two-Photon Induced Reactive Oxygen Species for Cell Damage. Nanomaterials (Basel). 2021;11:1180.
22. Chen Y, Zhang Y, Liang W, Li X. Gold nanocages as contrast agents for two-photon luminescence endomicroscopy imaging. Nanomedicine: Nanotechnology, Biology and Medicine. 2012;8:1267-1270.
23. Zhang Y, Liu AT, Cornejo YR, Van Haute D, Berlin JM. A Systematic comparison of in vitro cell uptake and in vivo biodistribution for three classes of gold nanoparticles with saturated PEG coatings. PLoS One. 2020; 15:e0234916.
24. Minaei SE, Khoei S, Khoee S, Mahdavi SR. Sensitization of glioblastoma cancer cells to radiotherapy and magnetic hyperthermia by targeted temozolomide-loaded magnetite tri-block copolymer nanoparticles as a nanotheranostic agent. Life Sciences. 2022;306:120729.
25. Wang Y, Zou L, Qiang Z, Jiang J, Zhu Z, Ren J. Enhancing Targeted Cancer Treatment by Combining Hyperthermia and Radiotherapy Using Mn-Zn Ferrite Magnetic Nanoparticles. ACS Biomater Sci Eng. 2020;6: 3550-3562.
26. Esmaeili Govarchin Ghaleh H, Zarei L, Mansori Motlagh B, Jabbari N. Using CuO nanoparticles and hyperthermia in radiotherapy of MCF-7 cell line: synergistic effect in cancer therapy. Artif Cells Nanomed Biotechnol. 2019; 47:1396-1403.
27. Jabbari N, Zarei L, Esmaeili Govarchin Galeh H, Mansori Motlagh B. Assessment of synergistic effect of combining hyperthermia with irradiation and calcium carbonate nanoparticles on proliferation of human breast adenocarcinoma cell line (MCF-7 cells). Artif Cells Nanomed Biotechnol. 2018;46:364-372.
28. Day ES, Bickford LR, Slater JH, Riggall NS, Drezek RA, West JL. Antibody-conjugated gold-gold sulfide nanoparticles as multifunctional agents for imaging and therapy of breast cancer. International journal of nanomedicine. 2010:445-454.
29. Ramezanzadeh E, Sadri K, Momennezhad M, Dolat E, Sazgarnia A. Evaluation of EGFR-targeted gold/gold sulfide (GGS) nanoparticles as a theranostic agent in photothermal therapy. Materials Research Express. 2018; 5:125401.
30. Sadat Shandiz SA, Shafiee Ardestani M, Shahbazzadeh D, Assadi A, Ahangari Cohan R, Asgary V, et al. Novel imatinib-loaded silver nanoparticles for enhanced apoptosis of human breast cancer MCF-7 cells. Artif Cells Nanomed Biotechnol. 2017;45:1-10.
31. Sadeghi HR, Bahreyni-Toosi MH, Meybodi NT, Esmaily H, Soudmand S, Eshghi H, et al. Gold-gold sulfide nanoshell as a novel intensifier for anti-tumor effects of radiofrequency fields. Iranian Journal of Basic Medical Sciences. 2014;17:516.
32. Li H, Beetsma L, Prakash S, Mikkers M, Botto L. Analysis and optimization of a multicascade method for the size fractionation of poly-dispersed particle systems via sedimentation or centrifugation. arXiv preprint arXiv:2303.05257. 2023.
33. Ma J, Li N, Wang J, Liu Z, Han Y, Zeng Y. In vivo synergistic tumor therapies based on copper sulfide photothermal therapeutic nanoplatforms Exploration, Wiley Online Library, pp 20220161.
34. Maestro LM, Haro-González P, Coello JG, Jaque D. Absorption efficiency of gold nanorods determined by quantum dot fluorescence thermometry. Applied Physics Letters. 2012;100.
35. Upadhyay C, Tripathy K, Bhattacharjee M. Scattering and Absorption Efficiency Analysis of Gold Nanospheres for Optoelectronic Applications 2024 8th IEEE Electron Devices Technology & Manufacturing Conference (EDTM), IEEE, pp 1-3.
36. Gobin AM, Watkins EM, Quevedo E, Colvin VL, West JL. Near-infrared-resonant gold/gold sulfide nanoparticles as a photothermal cancer therapeutic agent. Small. 2010;6:745-752.

37. Saifi MA, Khan W, Godugu C. Cytotoxicity of Nanomaterials: Using Nanotoxicology to Address the Safety Concerns of Nanoparticles. Pharm Nanotechnol. 2018;6: 3-16.

38. Dhiman S, Bakshi P, Kapoor N, Sharma P, Kohli SK, Mir BA, et al. Nanoparticle-Induced Oxidative Stress in Plant. Plant Responses to Nanomaterials: Recent Interventions, and Physiological and Biochemical Responses. 2021:269-313.

39. Vijayalakshmi S, Rajasekar A, Veeraraghavan VP, Ghidan AY, Al Antary TM, Karthikkumar V, et al. The pro-apoptotic and cytotoxic efficacy of polydatin encapsulated poly (lactic-co-glycolic acid)(PLGA) nanoparticles. Process Biochemistry. 2021;111:210-218.

40. Chang X, Wang X, Li J, Shang M, Niu S, Zhang W, et al. Silver nanoparticles induced cytotoxicity in HT22 cells through autophagy and apoptosis via PI3K/AKT/mTOR signaling pathway. Ecotoxicology and Environmental Safety. 2021;208:111696.

41. Al-Asiri WY, Al-Sheddi ES, Farshori NN, Al-Oqail MM, Al-Massarani SM, Malik T, et al. Cytotoxic and Apoptotic Effects of Green Synthesized Silver Nanoparticles via Reactive Oxygen Species–Mediated Mitochondrial Pathway in Human Breast Cancer Cells. Cell Biochemistry and Function. 2024;42:e4113.

42. Ramachandran R, Krishnaraj C, Kumar VA, Harper SL, Kalaichelvan TP, Yun SI. In vivo toxicity evaluation of biologically synthesized silver nanoparticles and gold nanoparticles on adult zebrafish: a comparative study. 3 Biotech. 2018;8:1-12.

43. Ghahremani FH, Sazgarnia A, Bahreyni-Toosi MH, Rajabi O, Aledavood A. Efficacy of microwave hyperthermia and chemotherapy in the presence of gold nanoparticles: an in vitro study on osteosarcoma. Int J Hyperthermia. 2011;27:625-36.

44. Mohammadi A, Hashemi B, Mehdi Mahdavi SR, Solimani M, Banaei A. Radiosensitization effect of radiofrequency hyperthermia in the presence of PEGylated-gold nanoparticles on the MCF-7 breast cancer cells under 6 MeV electron irradiation. J Cancer Res Ther. 2023;19:S67-S73.

45. PuY, Pons T. Gold Nanorod/Titanium Dioxide Hybrid Nanoparticles for Plasmon-Enhanced Near-Infrared Photoproduction of Hydroxyl Radicals and Photodynamic Therapy. ACS Applied Materials & Interfaces. 2023;15: 49943-49952.

46. Etemadi M, Golmohammadi S, Akbarzadeh A, Rasta SH. Plasmonic photothermal therapy in the near-IR region using gold nanostars. Applied Optics. 2023;62: 764-773.

47. Lo CY, Tsai SW, Niu H, Chen FH, Hwang HC, Chao TC, et al. Gold-nanoparticles-enhanced production of reactive oxygen species in cells at spread-out Bragg peak under proton beam radiation. ACS omega. 2023;8: 17922-17931.

48. Ma N, Wu FG, Zhang X, Jiang YW, Jia HR, Wang HY, et al. Shape-dependent radiosensitization effect of gold nanostructures in cancer radiotherapy: comparison of gold nanoparticles, nanospikes, and nanorods. ACS applied materials & interfaces. 2017;9:13037-13048.

49. Taheri A, Khandaker MU, Moradi F, Bradley DA. A simulation study on the radiosensitization properties of gold nanorods. Physics in Medicine & Biology. 2024;69: 045029.